Constructing Gradient Controllable Recurrent Neural Networks Using Hamiltonian Dynamics

Konstantin Rusch[1], John W. Pearson[2], and Konstantinos C. Zygalakis[2]

[1]Seminar for Applied Mathematics (SAM),
D-Math ETH Zürich,
Rämistrasse 101, Zürich-8092, Switzerland

[2]School of Mathematics,
University of Edinburgh,
Edinburgh, EH9 3FD, UK

November 2019

Abstract

Recurrent neural networks (RNNs) have gained a great deal of attention in solving sequential learning problems. The learning of long-term dependencies, however, remains challenging due to the problem of a vanishing or exploding hidden states gradient. By exploring further the recently established connections between RNNs and dynamical systems we propose a novel RNN architecture, which we call a *Hamiltonian recurrent neural network* (Hamiltonian RNN), based on a symplectic discretization of an appropriately chosen Hamiltonian system. The key benefit of this approach is that the corresponding RNN inherits the favorable long time properties of the Hamiltonian system, which in turn allows us to control the hidden states gradient with a hyperparameter of the Hamiltonian RNN architecture. This enables us to handle sequential learning problems with arbitrary sequence lengths, since for a range of values of this hyperparameter the gradient neither vanishes nor explodes. Additionally, we provide a heuristic for the optimal choice of the hyperparameter, which we use in our numerical simulations to illustrate that the Hamiltonian RNN is able to outperform other state-of-the-art RNNs without the need of computationally intensive hyperparameter optimization.

Keywords. recurrent neural networks (RNNs), deep learning, vanishing or exploding gradient, optimal parameter selection, Hamiltonian dynamics, sensitivity analysis

1 Introduction

Recurrent neural networks (RNNs) have recently achieved remarkable results in sequential learning problems, e.g. in speech recognition [11,12,26], computer vision [3,19,33] and time series prediction [7,9,25]. In this paper we focus on multiclass sequential learning problems, i.e. multiclass learning problems with time dependencies. Such learning problems can be formulated mathematically in the following way: Let $x_1, x_2, \dots, x_M \in \mathbb{R}^N$ be the training set of M time-dependent sequences $x_i = (x_i^0, x_i^1, \dots, x_i^N)$ of length N. Additionally, labels $y_1, y_2, \dots, y_M \in \{1, \dots, m\}$ are given for each x_i representing the class of the corresponding sequence. The goal is to learn a

function $\Phi : \mathbb{R}^N \to [0,1]^m$, where the j-th entry of $\Phi(x_i)$ represents the likelihood of sequence x_i belonging to class j, which minimizes a given functional on the training set (also known as the cost function). As we assume a-priori that there exist time dependencies in the training samples $\{x_i, y_i\}_{i=1}^N$, feedforward methods (such as convolutional neural networks [10,30] or support vector machines [8]) will probably fail to produce convincing solutions for this learning problem as they generally neglect time dependencies or autocorrelations in the underlying training sequences.

One approach to naturally include these time-dependencies in the learning procedure is through the use of RNNs, where recurrent weights exist between layers of the neural network. However, training RNNs on sequences with long-term dependencies remains a challenging problem. The issue hereby is that the gradient of the hidden states can go to zero or blow up to infinity exponentially, i.e. a vanishing or exploding gradient; see, e.g. [4, 27, 28] for a detailed description of that problem. As this gradient represents the influence of perturbations of a hidden state (and thus of an input) on the objective cost function, both a vanishing as well as an exploding gradient denotes a loss of information in the subsequent learning process.

Several approaches have been devised to solve this issue at least for very long sequences. One famous example in particular is the use of gating units in so-called Gated Neural Networks (GNNs) such as the Long Short-Term Memory (LSTM) [15] or the Gated recurrent unit (GRU) [6]. The gating mechanism controls the information which flows through a so-called memory cell and prevents therewith a vanishing gradient. However, an LSTM as well as a GRU can still suffer from exploding gradients [18]. Additionally, GNNs are computationally expensive, as they require more parameters than a plain RNN in general.

One very recent approach for analyzing the vanishing or exploding gradient problem is given in [13]. The authors derive a connection between deep neural networks and dynamical systems by interpreting a numerical approximation of an ordinary differential equation (ODE) as an architecture for a feedforward neural network. Each layer of the feedforward network is then described by the approximated solution of the ODE at a corresponding time level. Hence, solving the ODE for many time levels will result in very deep neural networks. Having established this link, the authors analyze the vanishing or exploding gradient problem using stability theory for the underlying dynamical system. This connection together with stability theory has already been used to construct an RNN architecture, the so-called Antisymmetric recurrent neural network (Antisymmetric RNN) [5]. The authors constrain the parameter space such that the underlying dynamical system will be stable by using antisymmetric matrices as the weight matrices of the RNN

We base our analysis on the same connection between deep neural networks and dynamical system. However, we construct novel RNN architectures using theory of Hamiltonian systems instead of stability theory. Therefore, since the underlying dynamical system of our RNN denotes a Hamiltonian system, we call it the Hamiltonian recurrent neural network (Hamiltonian RNN). Consequently we approximate this system with symplectic integrators in order to almost preserve its corresponding Hamiltonian at least for very long time intervals [14]. Based on this Hamiltonian model we are able to state an upper bound for the norm of the hidden states gradient which is causing the vanishing or exploding gradient. We subsequently show that the hidden states gradient can thus be controlled by a hyperparameter of the Hamiltonian RNN for a given sequential learning problem. Finally, in order to show the applicability of the proven upper bound of the hidden states gradient, we solve an inverse problem where we search for optimal hyperparameters of the Hamiltonian RNN for varying sequence lengths based on a simple exemplary learning problem. This supports the theoretical findings, which show that the hidden states gradient is of order $\mathcal{O}(1)$ (i.e. no vanishing or exploding gradient), if we choose the hyperparameter of the Hamiltonian RNN as the inverse of the sequence lengths.

The remainder of the paper is structured as follows. In Section 2 we discuss the problem

of vanishing or exploding gradients for vanilla RNNs, as well as discussing the connections between numerical integrators of ordinary differential equations and RNNs. Then, in Section 3, we analyze the continuous time properties of a Hamiltonian system similar to the one proposed in [13], and prove a bound for the sensitivity of the solution on the initial condition. We then propose an RNN based on the symplectic discretization of this Hamiltonian system and show numerically that it inherits the favorable long time properties of the continuous system. In particular, we show that the size of the hidden states gradient is controlled by a hyperparameter. This is explored further in Section 4, where we also provide a heuristic for the optimal choice of the hyperparameter. Numerical experiments using this choice of the hyperparameter are presented in Section 5, and clearly show the benefits of our approach when compared with state-of-the-art methods. We conclude in Section 6 with a summary and a discussion of future research directions.

2 Preliminaries

2.1 Vanishing or exploding gradient in vanilla RNNs

A plain (or vanilla) RNN can generally be defined in terms of the recursion of its hidden states. In the following we will consider RNNs with one hidden layer in which we have also recurrent connections. Hence, the RNN can be formulated by

$$\mathbf{h}_n = \sigma(\mathbf{W}\mathbf{h}_{n-1} + \mathbf{V}\mathbf{x}_{n-1} + \mathbf{b}), \qquad \mathbf{h}_i, \mathbf{b} \in \mathbb{R}^d, W \in \mathbb{R}^{d\times d}, \mathbf{x}_i \in \mathbb{R}^n, \mathbf{V} \in \mathbb{R}^{d\times n}, \tag{1}$$

where d is the number of neurons in the hidden layer and n is the dimension of the input, i.e. the number of features. We call $\mathbf{h}_i$ the hidden state at time i, $\mathbf{W}$ is the hidden weights matrix, $\mathbf{V}$ is the input weights matrix and $\mathbf{b}$ is the bias. The initial hidden state $\mathbf{h}_0$ is normally set to be the zero vector. As the hidden states are computed recursively, the standard backpropagation method cannot be applied for the subsequent learning process. However, a standard adaption of the backpropagation scheme for RNNs is the backpropagation through time (BPTT) method, where the hidden states are unfolded in time. Hence the RNN is treated as a feedforward network, where its number of hidden layers equals the length of the input sequences. For detailed motivation and description of the BPTT scheme we refer to [29, 32]. However, vanilla RNNs are generally avoided when it comes to sequential learning problems, as they tend to suffer from a vanishing or exploding gradient, e.g. numerical results in [2] and [21].

In order to define the vanishing or exploding gradient problem mathematically, let C be a suitable cost function of a given learning problem which we want to solve using RNNs. The gradient $\frac{\partial C}{\partial \mathbf{h}_i}$ then represents the dependence of the cost function on the hidden state $\mathbf{h}_i$. Furthermore, as the hidden state $\mathbf{h}_i$ depends on some input $\mathbf{x}_i$ at time t_i, the gradient also represents the dependence on the i-th input. However, if this gradient is (almost) zero, or tends to infinity, the information of input $\mathbf{x}_i$ and, because of the recursion, every previous input gets lost. The remaining question is now why the gradient typically goes to zero or to infinity. To answer this, is really useful to rewrite the gradient as

$$\frac{\partial C}{\partial \mathbf{h}_i} = \frac{\partial C}{\partial \mathbf{h}_N}\frac{\partial \mathbf{h}_N}{\partial \mathbf{h}_i} = \frac{\partial C}{\partial \mathbf{h}_N}\prod_{j=i}^{N-1}\frac{\partial \mathbf{h}_{j+1}}{\partial \mathbf{h}_j}.$$

We can then see that the gradient $\frac{\partial C}{\partial \mathbf{h}_i}$ can be represented as the product of $N - i + 1$ other gradients. If these are mostly bigger than 1 it will blow up, or it will go to zero if most of them are smaller than 1. Therefore, one is interested in RNNs where $\frac{\partial \mathbf{h}_N}{\partial \mathbf{h}_0}$ is a suitable constant $c \approx 1$.

2.2 Connection between dynamical systems and RNNs

The following connection between dynamical systems and neural networks is based on the theoretical concept provided by [13]. Note that the authors showed this connection for deep feed-forward networks only. We recall that the learning of RNNs can be reformulated as a forward problem using the BPTT scheme. Hence, the connection between dynamical systems and feed-forward networks can also applied to the recurrent case. As an example, [5] have recently used this link to construct novel RNN architectures. The cornerstone of connecting dynamical systems theory and neural networks is to interpret numerical approximations of a dynamical system as an RNN. To this end, let us examine the following differential equation:

$$\frac{\mathrm{d}\mathbf{h}}{\mathrm{d}t} = \sigma(\mathbf{W}\mathbf{h}(t) + \mathbf{b}), \quad \text{with } \mathbf{h}(0) = \mathbf{h}_0, \tag{2}$$

where $\mathbf{h}(t) \in \mathbb{R}^d, \mathbf{W} \in \mathbb{R}^{d\times d}, \mathbf{b} \in \mathbb{R}^d$, and σ is a sufficiently smooth and increasing function. Solving the differential equation (2) using a simple numerical integrator, for example the forward Euler method, yields the approximation

$$\mathbf{h}_{n+1} = \mathbf{h}_n + \epsilon\sigma(\mathbf{W}\mathbf{h}_n + \mathbf{b}), \tag{3}$$

where $\epsilon > 0$ is the time step of the numerical method. If we now interpret σ as an activation function, $\mathbf{W}$ as weights, $\mathbf{b}$ as a bias, and $\mathbf{h}_n$ as the hidden state at time t_n, equation (3) becomes an architecture for a specific RNN with an additional hyperparameter ϵ. This RNN has no input, as the underlying ODE (2) is autonomous. Also, in contrast to the standard (or vanilla) RNN, equation (3) has an additional feedback of the last computed hidden state $\mathbf{h}_n$ at every time step t_{n+1}. Note that this approach resembles the residual RNNs presented by [34]. The similarity is the skipping behavior, where the hidden state of the previous step gets fed back into the new hidden state. However, this architecture is based on a completely different idea and only the skipping part is the same.

One major benefit of this established connection is that we can now analyze the vanishing or exploding gradient problem in a continuous, dynamical systems set-up. We assume in the following that we can resemble the true dynamics of the system (2) using appropriate numerical integrators and rewrite the solution $\mathbf{h}$ of ODE (2) as $\mathbf{h}(t, \mathbf{h}_0)$ to emphasize the dependence of the solution on the initial value $\mathbf{h}_0$. Additionally, we recognize that the initial value $\mathbf{h}_0$ of the ODE (2) also denotes the initial hidden state of the RNN. Hence, differentiating $\mathbf{h}(t, \mathbf{h}_0)$ with respect to the initial value $\frac{\partial \mathbf{h}(t)}{\partial \mathbf{h}_0}$ denotes the continuous version of the hidden states gradient $\frac{\partial \mathbf{h}_n}{\partial \mathbf{h}_0}$ where $n = t/\epsilon$. As this gradient tends to go to zero or blows up to infinity, our goal is now to bound the continuous gradient $\frac{\partial \mathbf{h}(t)}{\partial \mathbf{h}_0}$ to overcome the problem of a vanishing or exploding gradient.

3 RNN with Controllable Hidden States Gradient

The basis of our novel RNN architecture is the following second-order equation:

$$\ddot{\mathbf{y}}(t) = \sigma(\mathbf{W}\mathbf{y}(t) + \mathbf{b}), \quad \text{with } \mathbf{y}(t_0) = \mathbf{y}_0, \tag{4}$$

where $\mathbf{y}(t) \in \mathbb{R}^d, \mathbf{W} \in \mathbb{R}^{d\times d}, \mathbf{b} \in \mathbb{R}^d$ and σ is a sufficiently smooth and increasing function as before. We can easily check that equation (4) is a Hamiltonian system with the corresponding Hamiltonian

$$H(\mathbf{z}, \mathbf{y}) = \frac{1}{2}\mathbf{z}^\top\mathbf{z} + f(\mathbf{y}), \quad \text{with } (\mathbf{z}, \mathbf{y}) \in Z \times Y \subseteq \mathbb{R}^d \times \mathbb{R}^d. \tag{5}$$

This can be done by simplifying the associated differential equations of Hamiltonian (5):

$$\begin{aligned}\frac{\mathrm{d}\mathbf{z}}{\mathrm{d}t} &= -\nabla_{\mathbf{y}} H(\mathbf{z}, \mathbf{y}) = -\nabla_{\mathbf{y}} f(\mathbf{y}),\\ \frac{\mathrm{d}\mathbf{y}}{\mathrm{d}t} &= \nabla_{\mathbf{z}} H(\mathbf{z}, \mathbf{y}) = \mathbf{z},\end{aligned}$$

to the second-order differential equation

$$\ddot{\mathbf{y}} = -\nabla_{\mathbf{y}} f(\mathbf{y}). \tag{6}$$

Assuming $\sigma(\mathbf{W}\mathbf{y}(t) + \mathbf{b})$ is in $L^1(Y)$, we can rewrite the right-hand side of equation (6) as the second-order equation (4), where

$$\nabla_{\mathbf{y}} f(\mathbf{y}) = -\int_Y \sigma(\mathbf{W}\mathbf{y}(t) + \mathbf{b})\, \mathrm{d}\mathbf{y}.$$

This Hamiltonian formulation allows to analyze the sensitivity of the solution with respect to the initial condition. In particular, if we consider $d = 1$, we can obtain an explicit bound on the growth of $\frac{\partial y}{\partial y_0}(t)$, where y_0 is the initial condition. This, again, yields a qualitative statement regarding the hidden states gradient of the corresponding RNN, which corresponds directly to the vanishing or exploding gradient problem.

We begin the sensitivity analysis by bounding the time derivative $\dot{y}(t)$.

Lemma 3.1. *Let $I = [0, T] \subset \mathbb{R}$ be a bounded interval. Additionally, let $y \in C^2(I; \mathbb{R})$ and $\sigma \in L^2(\mathbb{R})$ is bounded by $\sigma(x) \in [-1, 1]$ for all $x \in \mathbb{R}$. Consider the differential equation*

$$\ddot{y}(t) = \sigma(Wy(t) + b), \quad t \in I,$$

where $W, b \in \mathbb{R}$. The time derivative of y is then bounded by

$$-t + \dot{y}(0) \leq \dot{y}(t) \leq t + \dot{y}(0).$$

Proof. The proof is straightforward. Since σ is bounded by -1 and 1, we obtain the inequalities for $\ddot{y}$:

$$-1 \leq \ddot{y} \leq 1. \tag{7}$$

As the integral is a monotone operator we arrive at the following inequality by integrating both sides of (7):

$$\begin{aligned}&\int_0^t -1\, ds \leq \int_0^t \ddot{y}(s)\, ds \leq \int_0^t 1\, ds\\ \Leftrightarrow\quad &-t \leq \dot{y}(t) - \dot{y}(0) \leq t.\end{aligned}$$

□

Having proved this statement we are now able to state a bound for the norm of the solution to the Hamiltonian system (4) differentiated with respect to the initial solution in terms of the time variable. This denotes how the sensitivity of solution to (4) on the initial state $y(0)$ changes in time. We obtain this bound by deriving an equation which models the previously described sensitivity and bounding the norm of its solution afterwards.

Theorem 3.2. *Consider the same second-order differential equation as in Lemma 3.1 with its corresponding Hamiltonian*

$$H(\dot{y}, y) = \frac{1}{2}\dot{y}\dot{y} + f(y), \qquad f(y) = -\int_Y \sigma(Wy + b)dy$$

with initial values $y(0) = y_0$ *and* $\dot{y}(0) > T$*. The norm of the partial derivative* $\frac{\partial y}{\partial y_0}(t)$ *is then of order*

$$\left\| \frac{\partial y}{\partial y_0}(t) \right\| = \mathcal{O}(t).$$

Proof. Using the Hamiltonian property of preservation we obtain

$$H(\dot{y}, y) = \frac{1}{2}\dot{y}^2(t) + f(y(t)) = \frac{1}{2}\dot{y}^2(0) + f(y(0)).$$

Plugging in the definition for $f(y(t))$ yields

$$\frac{1}{2}\dot{y}^2(t) - \int_Y \sigma(Wy(t) + b)dy = \frac{1}{2}\dot{y}^2(0) + f(y(0)). \tag{8}$$

Differentiating both sides of equation (8) with respect to the initial state y_0 leads to

$$\begin{aligned} & \dot{y}\partial_t \frac{\partial y}{\partial y_0}(t) - \underbrace{\sigma(Wy(t) + b)}_{=\ddot{y}} \frac{\partial y}{\partial y_0}(t) = f'(y_0) \\ \Leftrightarrow\ & \partial_t \frac{\partial y}{\partial y_0}(t) - \frac{\ddot{y}(t)}{\dot{y}(t)} \frac{\partial y}{\partial y_0}(t) = \frac{f'(y_0)}{\dot{y}(t)} \\ \Leftrightarrow\ & \partial_t \frac{\partial y}{\partial y_0}(t) - \partial_t \log(\partial_t y(t)) \frac{\partial y}{\partial y_0}(t) = \frac{f'(y_0)}{\dot{y}(t)}. \end{aligned} \tag{9}$$

Using variation of parameters, we obtain the solution to (9):

$$\frac{\partial y}{\partial y_0}(t) = \dot{y}(t) \left(f'(y_0) \int_0^t \frac{1}{\dot{y}^2(s)} ds + \tilde{C} \right),$$

where $\tilde{C} \in \mathbb{R}$ is a constant. The norm of the gradient $\frac{\partial y}{\partial y_0}(t)$ can then be bounded by

$$\left\| \frac{\partial y}{\partial y_0}(t) \right\| \leq \|\tilde{C}\dot{y}(t)\| + \|f'(y_0)\dot{y}(t)\| \int_0^t \frac{1}{\dot{y}^2(s)} ds. \tag{10}$$

Using again that σ is bounded by -1 from below and thus $\ddot{y}(t)$ is bounded by -1 from below, we obtain the following lower bound on $\dot{y}(t)$:

$$\begin{aligned} & \dot{y}(t) \geq -t + \dot{y}(0) \\ \Rightarrow\ & \frac{1}{\dot{y}(t)^2} \leq \frac{1}{(\dot{y}(0) - t)^2}, \end{aligned}$$

since $\dot{y}(0) > T$ and hence $\dot{y}(0) > t$ for all $t \in I = [0, T]$. Plugging in this upper bound on $\dot{y}(t)^{-2}$ into the integral of (10) yields

$$\int_0^t \frac{1}{\dot{y}(s)^2} ds \leq \int_0^t \frac{1}{(\dot{y}(0) - s)^2} ds = \frac{1}{\dot{y}(0) - t} - \frac{1}{\dot{y}(0)} \leq \frac{1}{\dot{y}(0) - t}.$$

Therefore, using Lemma 3.1 we obtain the bound

$$\begin{aligned}\left\|\frac{\partial y}{\partial y_0}(t)\right\| &\leq \|\tilde{C}\dot{y}(t)\| + \|f'(y_0)\dot{y}(t)\|\frac{1}{\dot{y}(0)-t} \\ &\leq \|\tilde{C}\|(t+\dot{y}(0)) + \|f'(y_0)\|\frac{t+\dot{y}(0)}{\dot{y}(0)-t}.\end{aligned}$$

This concludes the claim that

$$\left\|\frac{\partial y}{\partial y_0}(t)\right\| = \mathcal{O}(t).$$

□

We can now use Theorem 3.2 to estimate the hidden state gradient of the corresponding RNN architecture which is causing the vanishing or exploding gradient problem. To this end we first need to derive the RNN architecture corresponding to the Hamiltonian system (4). When it comes to reasonably approximating Hamiltonian systems, special attention must be paid to the choice of numerical integrators. A natural such choice is the use of symplectic methods which are able to almost preserve the Hamiltonian at least for very long time intervals [**?**]. We will restrict ourselves to the standard second-order Leapfrog method to approximately solve the Hamiltonian system (4). However, higher-order splitting schemes can also be applied. Using the Leapfrog method yields the approximation

$$\begin{aligned}\mathbf{y}_1 &= \mathbf{y}_0 + \epsilon\tilde{\mathbf{y}}_0 + \frac{\epsilon^2}{2}\sigma(\mathbf{W}\mathbf{y}_0 + \mathbf{b}), \\ \mathbf{y}_{i+1} &= 2\mathbf{y}_i - \mathbf{y}_{i-1} + \epsilon^2\sigma(\mathbf{W}\mathbf{y}_i + \mathbf{b}), \qquad i = 1, \dots, N-1,\end{aligned} \tag{11}$$

where $\epsilon > 0$ is the time step of the method and $\mathbf{y}_0, \tilde{\mathbf{y}}_0$ are the initial values $\mathbf{y}(0)$ and $\dot{\mathbf{y}}(0)$. We interpret approximation (11) as an RNN with an additional hyperparameter ϵ and call it the Hamiltonian recurrent neural network (Hamiltonian RNN).
Using Theorem 3.2 we obtain $\|\frac{\partial y}{\partial y_0}(T)\| = \mathcal{O}(T)$. However, $T = N\epsilon$, where N is the length of the numerical approximation, and ϵ is the step size of the method. In the context of the Hamiltonian RNN N is the length of a sequence for a given sequential learning problem and ϵ is simply a hyperparameter of the architecture. Therefore we obtain the estimation

$$\left\|\frac{\partial y_N}{\partial y_0}\right\| = \mathcal{O}(N\epsilon).$$

This means for a given learning problem (i.e. a fixed N) we can linearly adjust the gradient $\|\frac{\partial y_N}{\partial y_0}\|$ with the hyperparameter ϵ such that the gradient will not vanish or explode. Note that the above estimation is independent of the RNN parameters, such as weights and bias, and thus holds also throughout the whole learning process.

Example 1. *We compute numerically the hidden states gradient* $\|\frac{\partial \mathbf{y}_N}{\partial \mathbf{y}_0}\|_2$ *for state space dimensions* $d = 1, 10, 100$. *In order to provide a general framework we initialize the Hamiltonian RNN parameters* $\{w_{ij}\}_{i,j=1}^d$ *and* $\{b_i\}_{i=1}^d$ *randomly using the standard initialization, i.e.* $\mathcal{U}([0, \frac{1}{d}])$ *distributions. Additionally we set* $\mathbf{y}(0) = \mathbf{0}$ *to be the zero vector, as this will also be the initial state for the corresponding RNN at the next step. The sequence length is set constantly to* $N = 1000$. *Using this parameter set-up Theorem 3.2 states that the hidden states gradient is of order* $\mathcal{O}(1000\epsilon)$, *where* ϵ *is the step-size of the numerical integrator used to solve the Hamiltonian system* (4). *Figure 1 shows the three resulting norms of the hidden states gradients for logscaled*

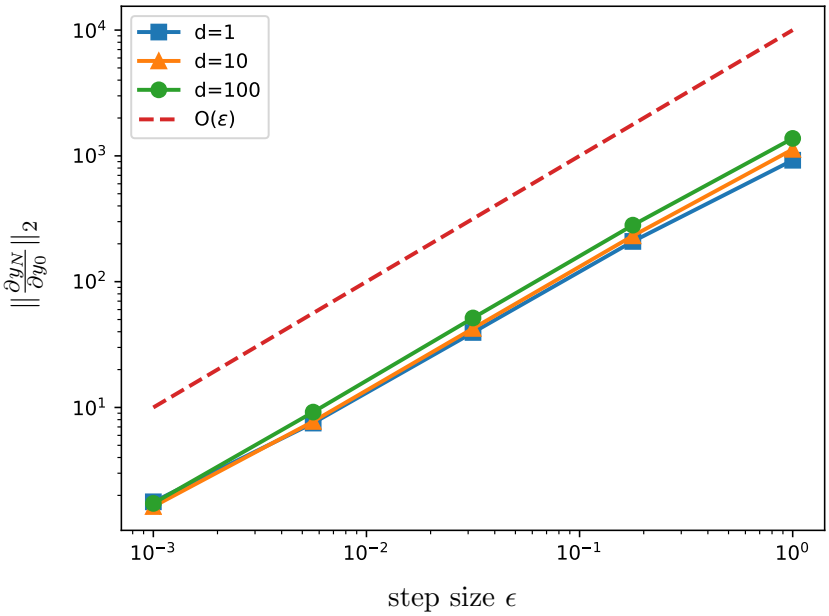

Figure 1: Numerically computed norm of hidden state gradients for different state space dimensions.

values of ϵ between 10^{-3} and 1. For $d = 1$ we can see the same behavior we proved in Theorem 3.2, i.e. the hidden states gradient scales linearly in ϵ. Additionally, even for much higher state space dimensions, the linear scalability of the hidden states gradient remains the same.

A natural question could be now what happens if we consider not the second-order system (4), but its first-order analogue instead:

$$\dot{\mathbf{y}}(t) = \sigma(\mathbf{W}\mathbf{y}(t) + \mathbf{b}), \quad \text{with } \mathbf{y}(0) = \mathbf{y}_0. \tag{12}$$

We investigate this numerically in the subsequent example.

Example 2. *We interpret the Euler integration of the first-order system* (12)

$$\mathbf{y}_{i+1} = \mathbf{y}_i + \epsilon\sigma(\mathbf{W}\mathbf{y}_i + \mathbf{b}), \qquad i = 1, \dots, N-1$$

again as an RNN architecture (Euler RNN). Figure 2 shows the numerically computed norm of the hidden states gradient $\|\frac{\partial y_N}{\partial y_0}\|_2$ of the Euler RNN for the same values of the RNN parameters as in the case of the Hamiltonian RNN. We can see that the gradient is unbounded and blows up exponentially with increasing values of ϵ, which would lead to an exploding gradient in the subsequent training process. Additionally, as we are generally not able to bound the exploding gradient, we cannot provide any heuristics of choosing the right hyperparameter ϵ. Nevertheless, [5] based their RNN architecture (Antisymmetric RNN) on the first-order system (12) *but with a solution approach to the exploding (or possibly vanishing) gradient in Figure 2. The authors connected the vanishing or exploding gradient to stability theory using the same link between RNNs and dynamical systems that we apply here. Their Antisymmetric RNN is based on the following system:*

$$\dot{\mathbf{y}}(t) = \sigma((\mathbf{W} - \mathbf{W}^\top - \gamma\mathbb{1})\mathbf{y}(t) + \mathbf{b}), \quad \textit{with } \mathbf{y}(0) = \mathbf{y}_0,$$

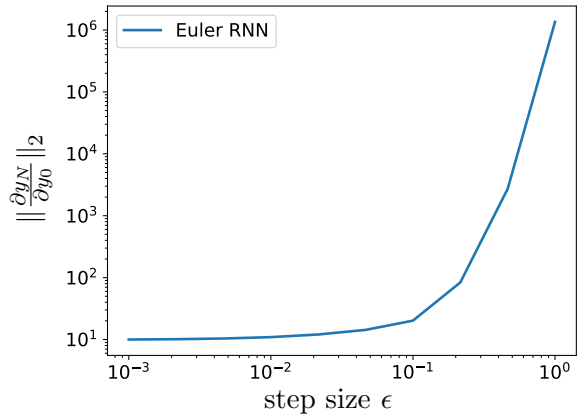

Figure 2: Exploding gradient of the first-order RNN.

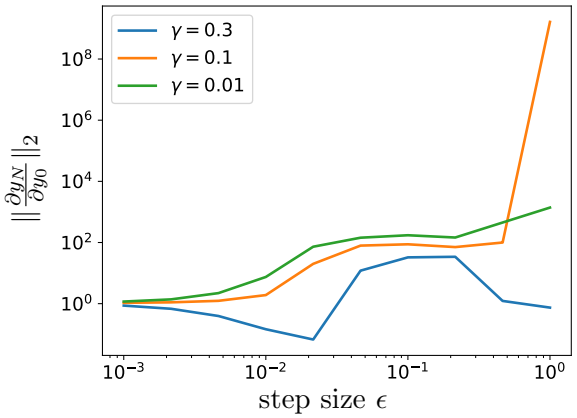

Figure 3: Influence of diffusion rate γ on the first-order RNN exploding gradient.

where $\mathbb{1}$ is the identity matrix and $\gamma > 0$ is a diffusion rate. This leads to an RNN with two additional hyperparameters, i.e. ϵ and γ. Figure 3 shows the similarly computed hidden states gradient as in Figure 2 but based on the Antisymmetric RNN for different values of the diffusion rate γ. We can see that for specific values of γ the gradient does not blow up exponentially. However, to our knowledge there exist no heuristics about the right choice of the two hyperparameters ϵ and γ such that the Antisymmetric RNN does not suffer from exploding or vanishing gradients. Moreover, the choice of the hyperparameters is tremendously sensitive to the subsequent learning success. Hence, a grid search algorithm with a very dense discretization has to be used in order to find suitable hyperparameters.

4 Optimal Trainability of the Hamiltonian RNN

So far the Hamiltonian RNN is not able to process any input as the underlying Hamiltonian system (4) is autonomous. To change this we have to add some weighted external force to (4) which makes it time dependent:

$$\ddot{\mathbf{y}}(t) = \sigma(\mathbf{W}\mathbf{y}(t) + \mathbf{V}\mathbf{x}(t) + \mathbf{b}), \qquad \text{with } \mathbf{y}(0) = \mathbf{y}_0, \tag{13}$$

where $\mathbf{y}(t), \mathbf{W}, \mathbf{b}$ and σ are exactly as in (4). However, $\mathbf{x}(t) \in \mathbb{R}^n$ is now the additional external force with weighting $\mathbf{V} \in \mathbb{R}^{d \times n}$. Applying the Leapfrog method to the time-dependent system (13) yields now the complete recursion formula for the Hamiltonian RNN:

$$\begin{aligned}
\mathbf{y}_1 &= \mathbf{y}_0 + \epsilon\tilde{\mathbf{y}}_0 + \frac{\epsilon^2}{2}\sigma(\mathbf{W}\mathbf{y}_0 + \mathbf{V}\mathbf{x}_1 + \mathbf{b}), \\
\mathbf{y}_{i+1} &= 2\mathbf{y}_i - \mathbf{y}_{i-1} + \epsilon^2\sigma(\mathbf{W}\mathbf{y}_i + \mathbf{V}\mathbf{x}_{i+1} + \mathbf{b}), \qquad i = 1, \dots, N-1,
\end{aligned}$$

where $\mathbf{x}_i = \mathbf{x}(t_i)$ is the RNN input at time step i.

Having established the connection between the hyperparameter ϵ of the Hamiltonian RNN and the hidden states gradient $\|\frac{\partial y_N}{\partial y_0}\|$, we are now interested in the learning performance of the Hamiltonian RNN depending on ϵ. We will base the subsequent numerical experiment on the following simple sequential learning problem. The Hamiltonian RNN reads in sequences $x = \{x_i\}_{i=1}^N$ of length $N > 0$ and generates a binary output after it processes the whole sequence.

A sequence x consists of independent standard Gaussian random variables $x_i \in \mathcal{N}(0,1)$ for all $i = 1, \dots, N$. The Hamiltonian RNN has to classify the sequences based on its mean, i.e. the mapping which has to be learned is

$$\Phi(x) = \begin{cases} 0 & \text{if } \mu(x) < 0, \\ 1 & \text{if } \mu(x) \geq 0, \end{cases} \qquad \text{with } \mu(x) = \frac{1}{N} \sum_{i=1}^{N} x_i.$$

The benefit of this experimental set-up is that we can easily adjust the length N of the given sequences. We are now interested in the optimal choice of the hyperparameter ϵ of the Hamiltonian RNN architecture for different lengths of the sequences which have to be learned.

However, before we start solving this inverse problem we first need to define optimality of the hyperparameter ϵ: Given a discretized interval $\mathcal{E} = 0 < \epsilon_1 < \epsilon_2 < \cdots < \epsilon_M$ with $M \in \mathbb{N}$ we call

$$\max_{\epsilon_i \in \mathcal{E}} \operatorname{acc}(\tilde{\Phi}_{\epsilon_i})$$

optimal, where acc is the accuracy of the Hamiltonian RNN approximation $\tilde{\Phi}_{\epsilon_i}$ of Φ using hyperparameter ϵ_i. In this case the number of weights and biases of the Hamiltonian RNNs are fixed, as well as their initialization. Additionally, the same training and test set is used as well as the same optimization method. Therefore this problem can be seen as inversely searching for an ϵ_i such that it maximizes the accuracy.

We solved this inverse problem with $M = 100$ equidistant values of ϵ between 0.01 and 1. We used the standard Adam optimization method ([20]) with a step size of 0.001 based on a stochastic mini-batch approach with mini-batch sizes of 100 and a training set (similarly test set) consisting of 1000 randomly generated sequences. Figure 4 shows the numerical results for

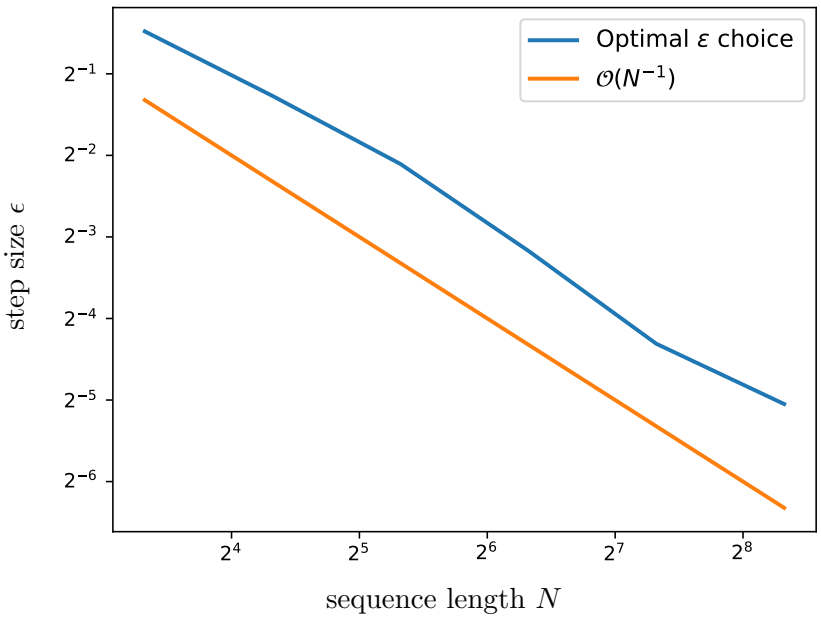

Figure 4: Optimal hyperparameter choices for the Hamiltonian RNN based on the Gaussian mean classification problem.

sequence lengths between 10 and 320. We can see that the optimal choice of ϵ scales linearly

with the length of the sequences N. We already proved that the choice $\epsilon = N^{-1}$ results in $\frac{\partial y_N}{\partial y_0} = \mathcal{O}(1)$ and thus no vanishing or exploding gradient is observed. Moreover, Figure 4 supports this numerically and shows that the optimal choice of the hyperparameter ϵ of the Hamiltonian RNN is given by

$$\epsilon = \mathcal{O}(N^{-1}). \tag{14}$$

5 Numerical Examples

The following experiments are implemented in the programming language Python, using NumPy [31] to represent the several RNNs. The differentiation of the code is done using the auto-differentiation library autograd [24]. The code is almost completely vectorized (besides the sequential functionality of RNNs) in order to increase performance. Additionally, the code is parallelized for efficient hyperparameter optimization methods using the Python library multiprocessing. The training of all RNNs is done similarly using mini-batch optimization together with the standard optimization routine Adam [20]. The plots are done using the Python graphics environment matplotlib [16]. We benchmark in the following experiments the Hamiltonian RNN against the Antisymmetric RNN as well as against the LSTM.

5.1 Normally distributed shock preservation

The goal of the first experiment is to measure how long information can be stored in an RNN. To this end, we construct a sequential learning problem where the RNN has to label some given sequences. These sequences are based on a straight line which is perturbed using normal distributions. In particular, sequences of class 0 are perturbed with a standard normal distribution only, but sequences of class 1 are heavily perturbed in the first few entries and perturbed using a standard normal distribution in all subsequent entries. Mathematically speaking, let

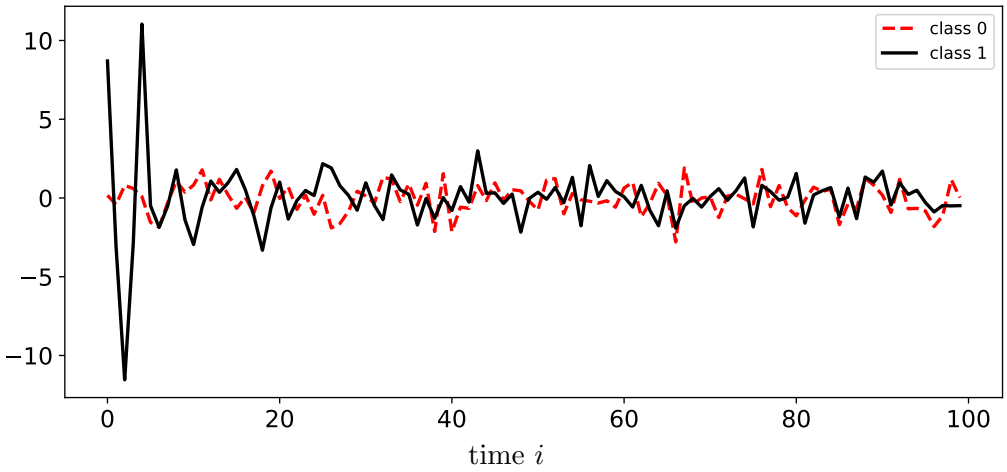

Figure 5: Exemplary sequences of both classes from the normal distributed shock preserving experiment.

$x^j = \{x_i^j\}_{i=1}^N$ be a sequence of class $j \in \{1, 2\}$. Then, $x_i^0 \in \mathcal{N}(0, 1)$ for all $i = 1, \dots, N$. Additionally, $x_i^1 \in \mathcal{N}(0, 1)$ for all $i = k + 1, \dots, N$, but $x_i^1 \in \mathcal{N}(0, 10)$ for all $i = 1, \dots, k$. We choose $k = 5$ in the following experiments. Figure 5 shows representative sequences for each individual class. Since the beginning of class 1 looks like a shock in the otherwise slightly perturbed

sequence, we call this experiment the normal distributed shock preservation. The objective for our RNNs is to correctly classify such sequences. This is done by feeding in one entry at a time to the RNN and generating one output after the RNN has seen the whole sequence. To speed up convergence a softmax layer is used for the output of the RNN. The minimization is done by using the cross-entropy cost function. We therefore define the accuracy of an RNN method as the percentage of correctly classified sequences in the test set.

We assume that an RNN has learned the problem when the accuracy is over 90%. We stop the learning process after it reaches this threshold. In order to fairly compare the different RNN architectures, we use a standard grid search algorithm to find a number of hidden neurons in combination with a learning rate for the optimization routine, which yield the fastest convergence to the accuracy threshold of 90%. However, only a further hyperparameter optimization has to be done for the Antisymmetric RNN, as we use the estimation (14) for an optimal choice of the hyperparameter ϵ of the Hamiltonian RNN.

Table 1: Number of hidden parameters for the shock preserving experiment.

		RNNs		
		LSTM	Anti. RNN	Ham. RNN
Length	100	10000	210	100
	500	22500	210	100
	2000	/	210	100
	5000	/	/	100

Table 1 shows the number of hidden parameters for each RNN architecture which yields the fastest convergence for the shock preserving experiment. Neglecting the bias, d neurons in the hidden states correspond to $4 \times d^2$ parameters in the LSTM, $d(d+1)/2$ parameters in the Antisymmetric RNN and d^2 parameters in the Hamiltonian RNN. Note that the missing numbers of hidden parameters in Table 1 denote the cases where no convergence is achieved for any combination of hyperparameters and for very long optimization processes. This is not to say that the RNNs would not eventually converge but more that for the given computational budget they fail to do so. In addition, we can conclude that the Hamiltonian RNN needs significantly less parameters than the other two RNNs and especially several orders of magnitude less than the LSTM.

Figure 6 shows the learning results for the shock preserving experiment for four different sequence lengths: $N = 100$, $N = 500$, $N = 2000$, and $N = 5000$. We plot the accuracy (based on the test set) against the learning iterations. Note that for visualization reasons the learning iterations are plotted using a log scale. We can see that for $N = 100$ the Hamiltonian RNN converges almost an order of magnitude faster than the Antisymmetric RNN. The LSTM needs an additional order of magnitude of iterations in order to converge. This behavior is reasonably similar for $N = 500$. The only difference here is that the LSTM needs even more parameters to converge at all. For $N = 2000$ only the Hamiltonian RNN and the Antisymmetric RNN demonstrate convergent behavior, and again the Hamiltonian RNN converges much earlier than the Antisymmetric RNN. Finally, for $N = 5000$ the Hamiltonian RNN is the only RNN architecture able to learn the underlying problem for the given computational budget. It is remarkable that the Hamiltonian RNN needs almost the same number of learning iterations to converge for every sequence length N as well as the exact same small number of hidden neurons, i.e. $d = 10$.

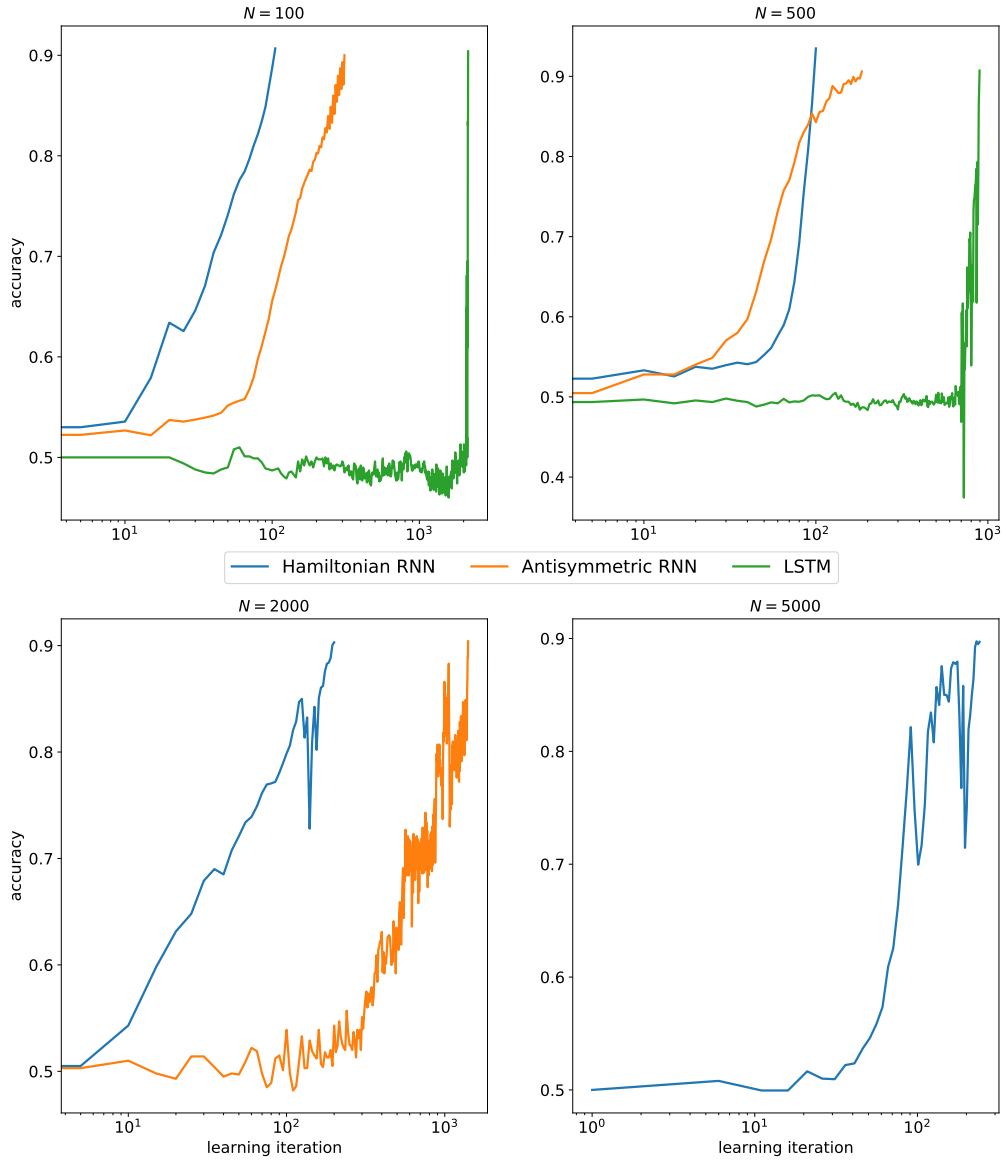

Figure 6: Learning results of the shock preserving experiment for four different sequence lengths.

5.2 Disturbed sequential XOR problem

In order to analyze how the different RNNs are able to solve non-trivial problems and preserve these outcomes for a long time, we introduce the following sequential learning problem. A sequence in the data set has length $N = 2 + \hat{N}$, where the first two entries are randomly initialized with 0 or 1 based on a discrete uniform distribution. The following $\hat{N}$ entries are uniform random numbers in $(0, 1)$. The goal of the learning algorithm is to correctly classify a

sequence based on the XOR output of the first 2 entries. Hence, let $x^j = \{x_i^j\}_{i=1}^N$ be a sequence of class $j \in \{1, 2\}$. Then, for the first two entries $x_1^j, x_2^j \in \mathcal{U}(\{0, 1\})$ of sequences of class j holds

$$x_1^j + x_2^j \mod 2 = j.$$

Additionally, $x_i^j \in \mathcal{U}([0, 1])$ for all $j = 1, 2$ and $i = 3, \ldots, N$. As the last $\hat{N}$ entries are only there to distract the RNN, the learning problem can be seen as solving a sequential learning problem and then storing the results for a long time (i.e. for time length $\hat{N}$) in the RNN. This is in contrast to the first experiment, where only information had to be stored. Table 2 shows the

Table 2: Number of hidden parameters for the sequential XOR experiment.

		RNNs		
		LSTM	Anti. RNN	Ham. RNN
Length	100	1600	210	100
	500	4900	210	100
	2000	19600	210	100
	5000	22500	210	100

number of hidden parameters which yields the fastest convergence for each RNN. This time all RNN architectures are able to learn the underlying problem for every sequence lengths: $N = 50$, $N = 100$, $N = 200$, and $N = 500$. However, while the number of parameters for the Hamiltonian RNN and the Antisymmetric RNN are comparable and very small, the number of parameters required by the LSTM is enormous.

Figure 7 shows the training results (in terms of accuracy) of the three RNN architectures for the four sequence lengths. We see that the Hamiltonian RNN and the Antisymmetric RNN behave very similarly, while the LSTM seems to have much more trouble to converge for $N \geq 200$. The learning iterations are plotted in linear scale here. We see that the LSTM needs approximately four times the number of iterations to converge for the sequence length of $N = 200$. Furthermore, it needs five times the number of learning iterations to converge compared to the RNN and Antisymmetric RNN for a sequence length of $N = 500$. Hence, we can conclude this experiment by pointing out that both the Hamiltonian RNN and the Antisymmetric RNN similarly outperform the LSTM in terms of the learning iterations required for convergence, as well as in terms of required number of parameters.

5.3 Sequential MNIST

The following experiment is based on the standard MNIST problem [22] in deep learning. The goal is to classify handwritten digits which are given as 28×28 grey-scale matrices. The training set consists of 60000 examples, and the test set consists of 10000 examples which vary in the difficulty of the classification. This problem was reformulated as a sequential learning problem in [21], where the $28 \times 28 = 784$ entries of one data sample are fed to an RNN one at a time. The feeding is done in scan-line order beginning at the top left of the matrix.

We train again the Hamiltonian RNN, the LSTM as well as the Antisymmetric RNN on this data set. Additionally, a simple grid search algorithm on suitable learning rates and number of hidden neurons is used for each RNN. However, only for the Antisymmetric RNN additional hyperparameter optimization is needed. The step-size hyperparameter ϵ of the Hamiltonian RNN is chosen accordingly to the estimation (14), i.e. inversely to the sequence length $N = 784$.

For the Antisymmetric RNN we do not beat the 90% line and obtain a maximum accuracy of 87%. Additionally, we obtain the same accuracy by using the LSTM as in [21], i.e. only

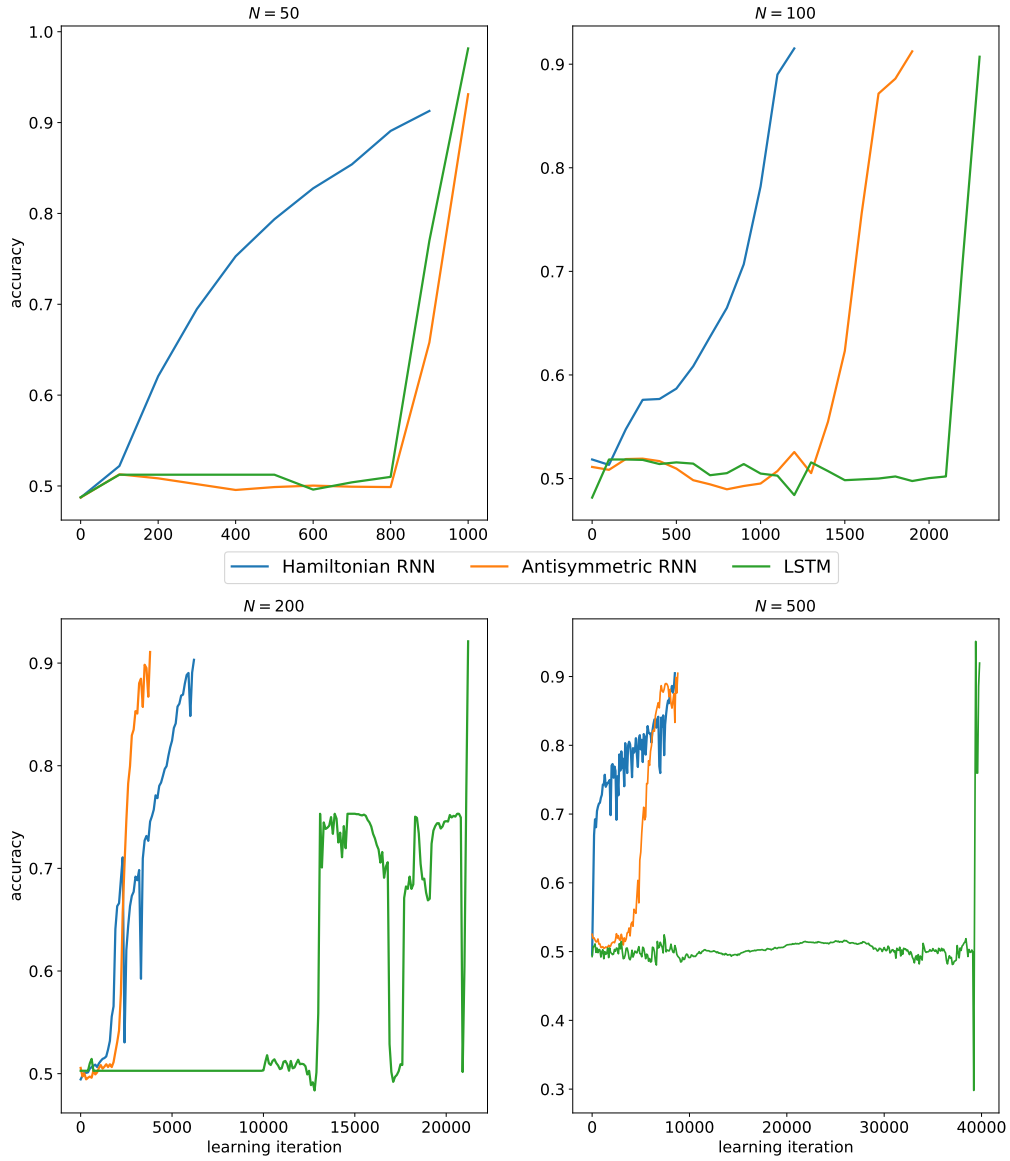

Figure 7: Learning results of the sequential XOR experiment for four different sequence lengths.

66%. The Hamiltonian RNN clearly outperforms both RNNs by reaching an accuracy of 94%. It is worth noting that our training procedure represents a plain optimization approach without any heavy fine-grid hyperparameter optimization or regularization of the RNNs to enhance performance. This is done in order to obtain a fair benchmark of the different architectures against each other. However, both methods the Antisymmetric RNN as well as the LSTM can perform notably better when more effort is put into the training process; see results in [2, 5].

6 Summary and Conclusion

In this paper we have addressed the issue of vanishing or exploding hidden states gradients for RNNs by constructing an RNN architecture where we can directly control the hidden states gradient. Using the link provided in [13] between deep neural networks and dynamical systems the new RNN was constructed by approximating a specific Hamiltonian system with symplectic integrators. Based on the Hamiltonian formulation we were able to demonstrate that the norm of the hidden states gradient is bounded linearly in time under certain assumptions on the initial values. Therefore, given a sequential learning problem (i.e. a fixed sequence length N), the gradient can then be linearly controlled by the step-size ϵ of the symplectic integrator. This means, however, in order to keep the hidden states gradient constant, the hyperparameter ϵ has to be chosen inversely to the sequence length. This consequently implies an estimation for the norm of the hidden states of $\mathcal{O}(1)$, and thus no vanishing or exploding gradient. To support this estimation numerically, we inversely solved for optimal ϵ values given a sequential learning problem with varying sequence lengths. It turned out that the optimal choice of the hyperparameter ϵ is indeed given by the estimation $\epsilon = \mathcal{O}(N^{-1})$. Additionally, we showed that using a first-order formulation of the same problem yields hidden states gradients which may blow up exponentially. Even though the Antisymmetric RNN in [5] fixes this problem by constraining the parameter space and adding an additional hyperparameter, a computationally heavy grid search algorithm has to be performed in order to find suitable hyperparameters.

In order to show the applicability of the Hamiltonian RNN we solved two exemplary sequential learning problems of academic nature based on self-generated training and test sets. We benchmarked the results to that of other state-of-the-art RNN architectures, i.e. the Antisymmetric RNN and the LSTM. Throughout all experiments the Hamiltonian RNN strictly outperformed the other RNNs by requiring less parameters for the optimization process. In particular, compared to the LSTM the Hamiltonian RNN required several orders of magnitude fewer parameters. Furthermore, we solved the MNIST problem which is widely used for benchmarking in deep learning. The Hamiltonian RNN again achieved a remarkably high accuracy compared to the LSTM and also to the Antisymmetric RNN.

In summary, using a plain optimization benchmarking framework, the Hamiltonian RNN strictly outperforms the other presented state-of-the-art RNN architectures. This, however, correlates with the provided heuristic of an optimal choice for the step-size hyperparameter of the Hamiltonian RNN.

Although the energy conserving property of Hamiltonian systems sounds attractive when it comes to constructing RNNs which do not suffer from information loss, complete conservation of information should still be avoided due to random noise in the underlying data sets. Therefore, one important future research topic is to analyze the Hamiltonian RNN applied to very noisy data sets. Additionally, we observed that Hamiltonian RNNs work surprisingly well in a data poor regime, i.e. having more network parameters than training samples. Using deep learning in the context of scientific computing leads often to a data poor regime, as generating data points is computationally highly expensive. Nevertheless, high accuracies still need to be obtained in these cases, see [23] for a detailed description and example of that problem. Building up on already presented work on generalization bounds for RNNs ([1, 17]), another important future research topic is to incorporate the special Hamiltonian design of the Hamiltonian RNN to explain its good generalization property even when having only few training samples.

Acknowledgement

KR was supported by the Helmholtz Association Initiative and Networking Fund under project number ZT-I-0003. Additional financial support was received by the University of Edinburgh, School of Mathematics through an MSc scholarship. JWP was supported by the Engineering and Physical Sciences Research Council (EPSRC) grant EP/S027785/1, and a Fellowship of the Alan Turing Institute. KCZ was supported by a Fellowship of the Alan Turing Institute. The computations of this work were done on the High-Performance Data Analysis (HPDA) cluster of the German Aerospace Center (DLR), Department of Simulation and Software Technology.

References

[1] Zeyuan Allen-Zhu and Yuanzhi Li. Can SGD learn recurrent neural networks with provable generalization? *arXiv preprint arXiv:1902.01028*, 2019.

[2] Martin Arjovsky, Amar Shah, and Yoshua Bengio. Unitary evolution recurrent neural networks. In *International Conference on Machine Learning*, pages 1120–1128, 2016.

[3] Shaojie Bai, J. Zico Kolter, and Vladlen Koltun. Trellis networks for sequence modeling. In *7th International Conference on Learning Representations (ICLR), New Orleans, LA, USA*, 2019.

[4] Yoshua Bengio, Patrice Simard, and Paolo Frasconi. Learning long-term dependencies with gradient descent is difficult. *IEEE Transactions on Neural Networks*, 5(2):157–166, 1994.

[5] Bo Chang, Minmin Chen, Eldad Haber, and Ed H. Chi. AntisymmetricRNN: A dynamical system view on recurrent neural networks. In *7th International Conference on Learning Representations (ICLR), New Orleans, LA, USA*, 2019.

[6] Kyunghyun Cho, Bart Van Merriënboer, Caglar Gulcehre, Dzmitry Bahdanau, Fethi Bougares, Holger Schwenk, and Yoshua Bengio. Learning phrase representations using RNN encoder-decoder for statistical machine translation. In *Proceedings of the 2014 Conference on Empirical Methods in Natural Language Processing (EMNLP)*, pages 1724–1734, 2014.

[7] Junyoung Chung, Kyle Kastner, Laurent Dinh, Kratarth Goel, Aaron C. Courville, and Yoshua Bengio. A recurrent latent variable model for sequential data. In *Advances in Neural Information Processing Systems*, pages 2980–2988, 2015.

[8] Corinna Cortes and Vladimir Vapnik. Support-vector networks. *Machine Learning*, 20(3):273–297, 1995.

[9] Marco Fraccaro, Søren Kaae Sønderby, Ulrich Paquet, and Ole Winther. Sequential neural models with stochastic layers. In *Advances in Neural Information Processing Systems*, pages 2199–2207, 2016.

[10] Kunihiko Fukushima. Neocognitron: A self-organizing neural network model for a mechanism of pattern recognition unaffected by shift in position. *Biological Cybernetics*, 36(4):193–202, 1980.

[11] Alex Graves. Sequence transduction with recurrent neural networks. *arXiv preprint arXiv:1211.3711*, 2012.

[12] Alex Graves, Abdel-rahman Mohamed, and Geoffrey Hinton. Speech recognition with deep recurrent neural networks. In *2013 IEEE International Conference on Acoustics, Speech and Signal Processing*, pages 6645–6649. IEEE, 2013.

[13] Eldad Haber and Lars Ruthotto. Stable architectures for deep neural networks. *Inverse Problems*, 34(1):014004, 2017.

[14] Ernst Hairer, Christian Lubich, and Gerhard Wanner. *Geometric numerical integration: structure-preserving algorithms for ordinary differential equations*. Springer-Verlag, Berlin and New York, 2002.

[15] Sepp Hochreiter and Jürgen Schmidhuber. Long short-term memory. *Neural Computation*, 9(8):1735–1780, 1997.

[16] John D Hunter. Matplotlib: A 2D graphics environment. *Computing in Science & Engineering*, 9(3):90–95, 2007.

[17] Haoming Jiang, Zhehui Chen, Minshuo Chen, Feng Liu, Dingding Wang, and Tuo Zhao. On computation and generalization of generative adversarial networks under spectrum control. In *7th International Conference on Learning Representations, ICLR 2019, New Orleans, LA, USA, May 6-9, 2019*, 2019.

[18] Sekitoshi Kanai, Yasuhiro Fujiwara, and Sotetsu Iwamura. Preventing gradient explosions in gated recurrent units. In *Advances in Neural Information Processing Systems*, pages 435–444, 2017.

[19] Andrej Karpathy and Li Fei-Fei. Deep visual-semantic alignments for generating image descriptions. In *Proceedings of the IEEE Conference on Computer Vision and Pattern Recognition*, pages 3128–3137, 2015.

[20] Diederik P. Kingma and Jimmy Ba. Adam: A method for stochastic optimization. In *3rd International Conference on Learning Representations (ICLR), San Diego, CA, USA*, 2015.

[21] Quoc V Le, Navdeep Jaitly, and Geoffrey E. Hinton. A simple way to initialize recurrent networks of rectified linear units. *arXiv preprint arXiv:1504.00941*, 2015.

[22] Yann LeCun, Léon Bottou, Yoshua Bengio, and Patrick Haffner. Gradient-based learning applied to document recognition. *Proceedings of the IEEE*, 86(11):2278–2324, 1998.

[23] Kjetil O Lye, Siddhartha Mishra, and Deep Ray. Deep learning observables in computational fluid dynamics. *arXiv preprint arXiv:1903.03040*, 2019.

[24] Dougal Maclaurin, David Duvenaud, and Ryan P. Adams. Autograd: Effortless gradients in NumPy. In *ICML AutoML Workshop*, volume 238, 2015.

[25] Pankaj Malhotra, Lovekesh Vig, Gautam Shroff, and Puneet Agarwal. Long short term memory networks for anomaly detection in time series. In *23rd European Symposium on Artificial Neural Networks, Computational Intelligence and Machine Learning, Bruges, Belgium*, 2015.

[26] Tomáš Mikolov, Martin Karafiát, Lukáš Burget, Jan Černockỳ, and Sanjeev Khudanpur. Recurrent neural network based language model. In *Eleventh Annual Conference of the International Speech Communication Association*, 2010.

[27] Razvan Pascanu, Tomas Mikolov, and Yoshua Bengio. Understanding the exploding gradient problem. *arXiv preprint arXiv:1211.5063*, 2012.

[28] Razvan Pascanu, Tomas Mikolov, and Yoshua Bengio. On the difficulty of training recurrent neural networks. In *International Conference on Machine Learning*, pages 1310–1318, 2013.

[29] David E. Rumelhart, Geoffrey E. Hinton, and Ronald J. Williams. Neurocomputing: Foundations of research. chapter Learning Representations by Back-Propagating Errors, pages 696–699. MIT Press, Cambridge, MA, USA, 1988.

[30] Karen Simonyan and Andrew Zisserman. Very deep convolutional networks for large-scale image recognition. In *3rd International Conference on Learning Representations (ICLR), San Diego, CA, USA*, 2015.

[31] Stefan Van Der Walt, S. Chris Colbert, and Gael Varoquaux. The NumPy array: a structure for efficient numerical computation. *Computing in Science & Engineering*, 13(2):22, 2011.

[32] Paul J. Werbos. Backpropagation through time: What it does and how to do it. *Proceedings of the IEEE*, 78(10):1550–1560, 1990.

[33] Kelvin Xu, Jimmy Ba, Ryan Kiros, Kyunghyun Cho, Aaron Courville, Ruslan Salakhudinov, Rich Zemel, and Yoshua Bengio. Show, attend and tell: Neural image caption generation with visual attention. In *International Conference on Machine Learning*, pages 2048–2057, 2015.

[34] Boxuan Yue, Junwei Fu, and Jun Liang. Residual recurrent neural networks for learning sequential representations. *Information*, 9(3):56, 2018.